

# POWER

## Technical Report 2018-13

Title: **Battery-Aware Contact Plan Design for LEO Satellite Constellations: The Ulloriaq Case Study**

Authors: Juan A. Fraire, Gilles Nies, Holger Hermanns, Kristian Bay, Morten Bisgaard

Report Number: 2018-13

ERC Project: Power to the People. Verified.

ERC Project ID: 695614

Funded Under: H2020-EU.1.1. – EXCELLENT SCIENCE

Host Institution: Universität des Saarlandes, Dependable Systems and Software  
Saarland Informatics Campus

Published In: IEEE GLOBECOM 2018

This report contains an author-generated version of a publication in IEEE GLOBECOM 2018.

**Please cite this publication as follows:**

Juan A. Fraire, Gilles Nies, Holger Hermanns, Kristian Bay, Morten Bisgaard.  
*Battery-Aware Contact Plan Design for LEO Satellite Constellations: The Ulloriaq Case Study.*  
IEEE Global Communications Conference, GLOBECOM 2018, Abu Dhabi, United Arab Emirates,  
December 9-13, 2018. IEEE 2018, ISBN 978-1-5386-4727-1. 1-7.



# Battery-Aware Contact Plan Design for LEO Satellite Constellations: The Ulloriaq Case Study

Juan A. Fraire\*, Gilles Nies†, Holger Hermanns†, Kristian Bay‡, Morten Bisgaard‡

\*CONICET - Universidad Nacional de Córdoba, Córdoba, Argentina

†Saarland University, Saarland Informatics Campus, Saarbrücken, Germany

‡GomSpace A/S, Aalborg, Denmark

**Abstract**—Power demands of communication technologies between LEO small-satellites are difficult to counterbalance by solar infeed and on-board battery storage, due to size and weight limitations. This makes the problem of battery-powered inter-satellite communication a very difficult one. Its management requires a profound understanding as well as techniques for a proper extrapolation of the electric power budget as part of the inter-satellite and satellite-to-ground communication design. We discuss how the construction of contact plans in delay tolerant networking can profit from a sophisticated model of the on-board battery behavior. This model accounts for both nonlinearities in battery behavior as well as stochastic fluctuations in charge, so as to control the risk of battery depletion. We take an hypothetical Ulloriaq constellation based on the GOMX-4 satellites from GomSpace as a reference for our studies.

## I. INTRODUCTION

There is an increasing interest of the space community in deploying large-scale Low-Earth Orbit (LEO) networks with the purpose of providing timely access to information [1]. In-orbit satellites such as the GOMX-4A and GOMX-4B satellites from GomSpace are already pushing for new space-terrestrial communication techniques and technologies capable of efficiently moving data between space and ground networks. Indeed, real-time access to data is only feasible when a chain of links between ground and (potentially several) satellites align to reach a remote destination. As illustrated in Figure 1, the lowest datarate on the chain, typically inter-satellite links, becomes the throughput bottleneck. Consequently, communication resources tend to remain largely underutilized.

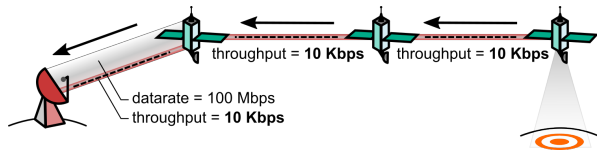


Figure 1. Low datarate inter-satellite links become the throughput bottleneck of real-time traffic. In this example, the space-to-ground link, typically faster because of resources such as large antennas on ground, is only utilized 0.01%

In this context, Delay Tolerant Networking (DTN) has been identified as a disruptive approach which allows for a better utilization of communication opportunities by means of storing, carrying and forwarding data [2]. Store, carry and forward enables a full utilization of available data rate and allows non-latency-constrained data to flow even when the destination

is not directly reachable. Therefore, satellites in orbit can prepare data in advance via longer but slower communication opportunities, making an efficient use of shorter but faster downlink opportunities with ground. However, it is crucial to have detailed knowledge on how much power is drained for satellite-to-ground and inter-satellite links, especially when in eclipse, where on-board batteries possibly end up in critically low states of charge. DTN is a perfect fit for this problem as on-board communication subsystems can be scheduled to meet local power resources. Specifically, each satellite's transponder's duty cycle can be embedded into a mutual contact plan, which is computed and designed in advance to provide optimal data delivery throughput and latency [3].

Previous work on the contact plan design problem for DTN satellite networks focused on fairness [4], routing [5], and scheduled traffic [6] or mission tasks [7], but none of them has considered the battery load and constraints. On the other hand, authors had addressed the battery-aware task scheduling problem for LEO satellites [8], [9], but the proposed approach assumed a single (non-networked) satellite. Indeed, the impact on the battery charge of inter-satellite transponders used for in-orbit networking has far been disregarded. To tackle this constellation-wide problem, we propose a Mixed Integer Linear Programming (MILP) model comprising store and forward network flow and linear battery abstractions from which battery-aware communication schedules can be derived. The model is validated with realistic battery models in a possible configuration of the Ulloriaq constellation, based on the GOMX-4A and GOMX-4B satellites.

This paper is structured as follows. An overview of the Ulloriaq case study, the battery model and the battery-aware scheduling procedure are given in Section II. In particular, relevant energy storage models are investigated in Section II-B. Results are analyzed and discussed in Section III. Conclusions are finally summarized in Section IV.

## II. SYSTEM MODEL

### A. Ulloriaq Constellation Overview

GOMX-4A and 4B, launched on February 2017, are 6U CubeSat from GomSpace, commissioned by the Danish Ministry of Defense and the European Space Agency. The overall mission focuses on demonstrating miniaturized technologies, namely orbit maintenance, inter-satellite links, high speed downlink and advanced sensing. These are considered key

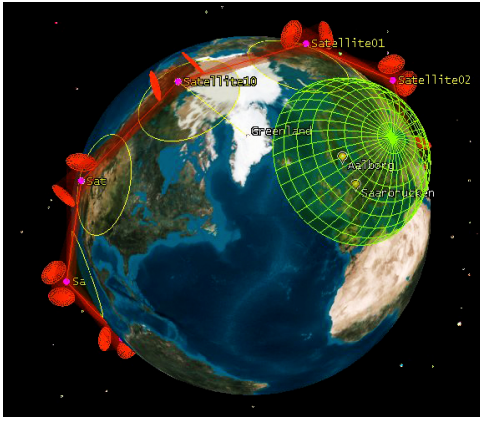


Figure 2. The proposed configuration for the Ulloriaq constellation

building blocks for a controlled deployment, operation and maintenance of a future CubeSat-based constellation known as Ulloriaq (the Greenlandic word for “star”). The potential Ulloriaq mission could be aimed at collecting observation and remote sensing data over the Greenland territory to deliver it to a ground station located in Aalborg, Denmark. The proposed space segment is composed of 10 satellites equally separated in the same orbital plane flying in an along-track formation, also known as train formation. As illustrated in Figure 2, the constellation aims at forming a ring around the Earth with a high revisit rate over Greenland territory. As in GOMX-4 mission, satellites are provisioned with two inter-satellite antennas pointing to the front and back neighbor, which allows to timely and cooperatively relay sensed data to the Aalborg ground station.

Table I specifies the ground, orbital and datarate parameters assumed for the Ulloriaq constellation in this study. The latitude and longitude given for the Greenland territory correspond to the centroid of a target area composed of

Table I  
ULLORIAQ CONSTELLATION PARAMETERS

Ground Segment				
Id		Lat. [deg]	Lon. [deg]	Notes
G	Greenland	73.25	-42.53	Area has 12750 points
A	Aalborg	57.05	9.93	38.53 m of altitude

Space Segment						
Id	Name	Inc. [deg]	RAAN [deg]	T. Anom. [deg]	Avg. Height [km]	Notes
1	Sat1	97.56	168.87	0	540	HSL
2	Sat2	97.56	168.87	36	540	
3	Sat3	97.56	168.87	72	540	
4	Sat4	97.56	168.87	108	540	
5	Sat5	97.56	168.87	144	540	
6	Sat6	97.56	168.87	180	540	HSL
7	Sat7	97.56	168.87	216	540	
8	Sat8	97.56	168.87	252	540	
9	Sat9	97.56	168.87	288	540	
10	Sat10	97.56	168.87	324	540	

Greenland to Sat	Sat to Sat	Sat to Aalborg
10 kbps	10 kbps	100 Mbps (HSL)

12750 boundary points that mimic the sensing area. The listed orbital parameters describe a heliosynchronous orbit for each of the 10 satellites, a desired property that guarantees periodic sunlight exposure and eclipse episodes for the constellation. It is also assumed that only two satellites (Sat1 and Sat6) are equipped with a high speed downlink (HSL) transponder. In order to reach the ground station in Aalborg, Denmark via high-speed-link, the data may need to be relayed between satellites via inter-satellite links. However, to properly decide how and when links should be used, battery utilization must be considered.

### B. Linear Battery Model vs. Kinetic Battery Model

In order to reason about energy consumption we need a faithful formal representation of energy storage in satellites. In the majority of cases Li-ion battery packs are used in CubeSat missions. Ulloriaq will be no exception. We introduce two battery models that are often used in that context and considered in this work. A thorough comparison of state-of-the-art formal battery models can be found in [10].

a) *Linear Battery Model*: The *Linear Battery Model* (LiBaM) is arguably the most used and simple model of energy storage. It is often thought of as a well holding fluid that can be drained or refilled as seen in Figure 3. Let  $\ell(t)$  be a piecewise constant function, representing the load on the battery. Then, the battery’s state of charge  $e(t)$  evolves piecewise linearly over time  $t$  and proportionally to  $\ell(t)$ , i.e.  $\dot{e}(t) = \ell(t)$ , where  $\dot{e}$  is the time derivative of  $e$ . The load represents charging and discharging if  $\ell(t) < 0$  and  $\ell(t) > 0$ , respectively. We consider the battery to be critical if  $e(t) \leq c_{\min}$ , where  $c_{\min} \geq 0$  is referred to as the *safe* threshold. The model can be extended easily by a capacity limit  $c_{\max}$ : If  $e(t)$  hits  $c_{\max}$  during a charging period, it simply remains at  $c_{\max}$  for the remainder of that period. Batteries are however inherently non-linear, thus the LiBaM is an unjustifiably optimistic model of energy storage.

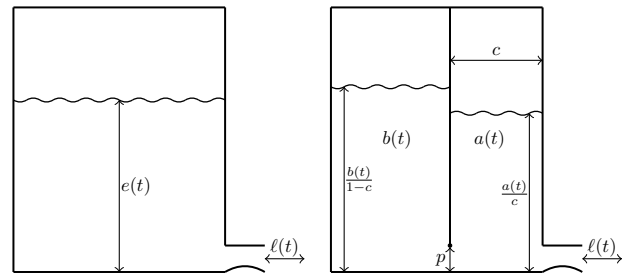


Figure 3. The one-well representation of the linear battery model (left) and the two-wells representation of the kinetic battery model (right).

b) *Kinetic Battery Model (KiBaM)*: The *Kinetic Battery Model* (KiBaM) improves over the LiBaM by splitting the stored charge into two portions, namely (i) the available charge  $a(t)$ , that is directly affected by the load on the battery, and (ii) the bound charge  $b(t)$ , that is not directly influenced by the load, but is rather chemically bound inside the battery. Bound charge is converted into available charge over time

(or vice-versa) via diffusion from one well to the other. The diffusion speed is regulated by the non-negative parameter  $p$  and is proportional to the difference in height of both wells, while  $c \in [0, 1]$  specifies the fraction of available charge. The KiBaM is often depicted as two interconnected wells holding fluid (see Figure 3). Mathematically, the KiBaM follows two coupled differential equations:  $\dot{a}(t) = -\ell(t) + p \cdot (b(t)/(1-c) - a(t)/c)$  and  $\dot{b}(t) = p \cdot (a(t)/c - b(t)/(1-c))$ . The dynamics of the KiBaM account for a couple of non-linear effects that can be observed on real-world batteries, like the *recovery effect* and the *rate-capacity effect*, both rooted in the relatively slow conversion of bound charge into available charge. The battery is assumed to be at a critically low charge level if the available charge drops to or below a safety threshold  $c_{\min}$ , i.e. if  $a(t) \leq c_{\min}$ . Notably, even for  $c_{\min} = 0$  some energy will be left in the battery in chemically bound form on hitting the threshold. The KiBaM has been extended by capacity limits as well as stochastic fluctuations in charge and loads [11] in order to get tight bounds on battery depletion risks in cases when the initial state of charge might be uncertain. For the work presented here it suffices to introduce the visualization of these so called State of Charge (SoC) distributions along a sequence of load distributions. For a detailed and rigorous treatment of this *stochastic* KiBaM we refer to [11].

A SoC distribution is displayed as two parts, namely (i) a heatmap representing the probability density function of the two-dimensional KiBaM SoC on the range from depletion to the battery capacity limits, with the available and bound charge on the  $y$ -axis and  $x$ -axis respectively, and (ii) the accumulated depletion risk as a color coded probability value. Figure 4 depicts the evolution of an exemplary SoC distribution along an exemplary load sequence.

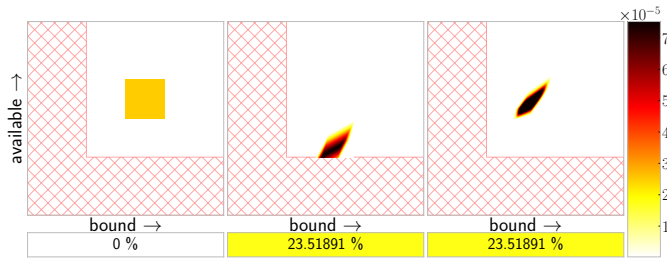


Figure 4. **Left:** An exemplary KiBaM SoC distribution ( $c = 0.5$ ,  $p = 0.05$ ,  $c_{\max} = 200$ ,  $c_{\min} = 30$ ) with an uniformly distributed initial SoC over the area  $[50, 70] \times [50, 70]$ . The unsafe region (below  $c_{\min}$ ) is represented as red hatched areas. **Middle:** After discharging for 6 time units with a noisy load of 5.5 whose noise model is a truncated Gaussian with support  $[-1, 1]$ . Roughly 23.5% of the probability mass depletes and is accumulated in the bottom part, where it remains. **Right:** After charging the remaining 74.5% for 3 time units with a load of  $-7$ .

### C. Mixed-Integer Linear Programming Model

In order to tackle the battery-aware link scheduling problem for DTN satellite networks, we consider an abstraction of the satellite constellation based on a discrete set of time episodes where the topology is considered stable and can be modeled by a temporary static graph. As thoroughly discussed in [6], a

set of  $K$  states, each of them comprised of a static graph with  $N$  nodes valid during a specific period of time  $((t_k; t_{k+1}))$ , can be used to represent the time-evolving network connectivity. In other words, whenever a communication opportunity starts or ends, a new state is added to the topology to describe the new connectivity. However, in a battery-aware model, a state change is also triggered by a change from sunlight exposure to eclipse, since it represents a transition from charging to discharging (and vice-versa) of the on-board batteries. Auxiliary coefficients such as contact capacity  $(\{c_{k,i,j}\})$ , buffer capacity  $(\{b_i\})$  and traffic sources  $(\{d_k^{i,j}\})$  can be used to complete the abstraction of the satellite constellation. It is worth noticing that in this work, buffer limits are set high enough in order to avoid memory congestion problems. Battery coefficients are included as part of the model and specified by the minimum and maximum battery charge allowed  $(\{c_{\min,i}\}$  and  $\{c_{\max,i}\})$  as well as the initial charge  $(\{c_{0,i}\})$ . The battery is recharged only if the spacecraft is currently exposed to sunlight by the difference of the solar infeed  $(\{c_{rC}^i\})$  and the link activity (given by  $\{c_{rT}^i\}$  and  $\{c_{rB}^i\})$ . As output variables we designate the traffic flowing through the network  $(\{X_{k,i,j}^{y,z}\})$ , the buffer occupancy as states evolve  $(\{B_{k,i}^{y,z}\})$ , link utilization variables  $(\{Y_{k,i,j}\})$ , and the LiBaM state of charge at the end of each state  $(\{C_{k,i}\})$ . Model parameters are summarized in Table II.

A Mixed-Integer Linear Programming (MILP) model can be specified based on these coefficients and variables. Equations (2) to (7) are the constraints of a time-evolving statement

Table II  
MILP MODEL PARAMETERS

Input Coefficients	
$N$	Nodes quantity
$K$	Topology states quantity
$\{t_k\}$	State $k$ start time ( $1 \leq k \leq K$ )
$\{i_k\}$	State $k$ duration ( $i_k = t_k - t_{k-1} : 1 \leq k \leq K$ )
$\{x_{k,i,j}\}$	Capacity of $i$ to $j$ contact at state $k$ ( $1 \leq k \leq K$ and $1 \leq i, j \leq N$ )
$\{b_{\max,i}\}$	Maximum buffer capacity at node $i$ ( $1 \leq i \leq N$ )
$\{d_k^{i,j}\}$	Traffic from $i$ to $j$ originated at the beginning of $k$ ( $1 \leq k \leq K$ and $1 \leq i, j \leq N$ )
$\{p_i\}$	Max. simultaneous links in node $i$ ( $1 \leq i \leq N$ )
$M$	Big "M" coefficient for interface decision equations
$\{c_{\min,i}\}$ $\{c_{\max,i}\}$	Minimum and maximum battery charge at node $i$ ( $1 \leq i \leq N$ ) at all times
$\{c_{0,i}\}$	Initial battery charge at node $i$
$\{c_{rC}^i\}$	Battery recharge rate because of sunlight exposure at node $i$ , if on eclipse, then this coefficient shall be 0
$\{c_{rT}^i\}$	Battery consumption rate because of transmission or reception system enabled at node $i$
$\{c_{rB}^i\}$	Battery consumption rate because of background load at node $i$
Output Variables	
$\{X_{k,i,j}^{y,z}\}$	Traffic from $y$ to $z$ at state $k$ flowing in $i$ to $j$ edge ( $1 \leq i, j, y, z \leq N$ )
$\{B_{k,i}^{y,z}\}$	Node $i$ buffer occupancy at the end of state $k$ by the traffic flow from $y$ to $z$ ( $1 \leq i, y, z \leq N$ )
$\{Y_{k,i,j}\}$	Binary variable for link selection from $i$ to $j$ at state $k$ ( $1 \leq k \leq K$ and $1 \leq i, j \leq N$ )
$\{C_{k,i}\}$	Battery charge at node $i$ at the end of state $k$ ( $1 \leq k \leq K$ and $1 \leq i, j \leq N$ )

$$\text{minimize: } \sum_{k=1}^K \sum_{i=1}^N \sum_{j=1}^N \sum_{y=1}^N \sum_{z=1}^N w(t_k) \cdot X_{k,i,j}^{y,z} + Y_{k,i,j} - C_{k,i} \quad (1)$$

Subject to:

$$\sum_{j=1}^N X_{k,j,i}^{y,z} - \sum_{j=1}^N X_{k,i,j}^{y,z} = B_{k,i}^{y,z} - (B_{k-1,i}^{y,z} + d_k^{i,z}) \quad \forall k, i, y, z \quad (2)$$

$$B_{k,i}^{y,z} \leq b_{\max}^i \quad \forall k, i, y, z \quad (3)$$

$$B_{0,i}^{y,z} = 0 \quad \forall i, y, z \quad (4)$$

$$\sum_{y=1}^N \sum_{z=1}^N X_{k,i,j}^{y,z} \leq x_{k,i,j} \quad \forall k, i, j \quad (5)$$

$$\sum_{k=1}^K \sum_{j=1}^N X_{k,i,j}^{y,z} = \sum_{k=1}^K d_k^{i,j} \quad \forall i = y, z \quad (6)$$

$$\sum_{k=1}^K \sum_{i=1}^N X_{k,i,j}^{y,z} = \sum_{k=1}^K d_k^{i,j} \quad \forall y, j = z \quad (7)$$

$$\sum_{j=1}^N Y_{k,i,j} \leq p_i \quad \forall i, k \quad (8)$$

$$\sum_{j=1}^N \sum_{y=1}^N \sum_{z=1}^N X_{k,i,j}^{y,z} \leq M \cdot Y_{k,i,j} \quad \forall i, k \quad (9)$$

$$C_{0,i} = c_{0,1} \quad \forall i \quad (10)$$

$$c_{\min}^i \leq C_{k,i} \leq c_{\max}^i \quad \forall k, i \quad (11)$$

$$C_{k,i} \leq C_{k-1,i} + (c_{rC}^i - c_{rB}^i - c_{rT}^i \sum_{j=1}^N Y_{k,i,j}) \cdot t_k \quad \forall k, i \quad (12)$$

of the known multi-commodity flow problem which has already been applied for store, carry and forward satellite networks in [6]. Specifically, equation (2) models the evolution of data as it either flows between nodes ( $\{X_{k,i,j}^{y,z}\}$ ) or is kept in a local storage ( $\{B_{k,i}^{y,z}\}$ ). Equations (3) and (4) specifies the maximum and initial status of each node's buffer. Equation (5) specifies the maximum flow of data that can be sent over each contact. Equations (6) and (7) set the flow imbalance, or traffic demands ( $d_k^{i,j}$ ) from all source to destination nodes.

The rest of the equations specifies resources limitations to the former flow model. Equations (8) and (9) provide a mechanism to bound the maximum quantity of simultaneous communications a given node can establish at any given moment. In this work, we have set  $p_i = 3$  meaning that at most two inter-satellite links and one ground station link can be used. Equation (10) is used to set the initial battery state of charge, Equation (11) bounds the battery charge at all states and Equation (12) models the evolution of charge throughout states using the LiBaM. Given these constraints,

the objective function in 1 aims at obtaining an optimal traffic flow assignment, where later flows are penalized by a  $w(t_k)$  cost function that increases with time.

As a result, an optimal traffic assignment can be obtained, and a battery-aware contact plan can be provisioned to the constellation to enable the utilization of communication resources while minimizing battery exhaustion probability. Unfortunately, although the MILP model includes the LiBaM formulation, the latter might not accurately reflect the real battery behavior, which is not linear. However, the KiBaM cannot be expressed within the MILP due to its non-linearity. As to be discussed in Section III, safe margins shall thus be considered when using the linear model. As an additional quality assurance and potential refutation mechanism, the contact plan synthesized with the LiBaM included in the MILP can be validated using the vastly more accurate stochastic KiBaM in a post-processing step. This is indeed what we do.

### III. RESULTS AND ANALYSIS

We set the model based on the Ulloriaq connectivity and feed it with a total of 187.5 MB (1500 Mbit) of data to be transmitted from the Greenland territory at the beginning of a 48 hs analysis window. The scenarios and the resulting contact plans were generated using the System Tool Kit (STK) and the Contact Plan Designer plug-in [12]. The contact topology comprising all possible communication opportunities is presented in Figure 5 and requires of a model of  $k = 1240$  states. It is evident that even though inter-satellite communications (in red) could be enabled at any time during sunlight and eclipse periods, it becomes prohibitive from a power budget perspective. Figure 6 illustrates the contact plan where only direct, or non-store-carry-and-forward data flow is present between Aalborg and Greenland. Although any satellite's batteries would hardly deplete on such a low transponder utilization, a DTN approach is appealing to increase the overall data delivery at higher latencies.

Two possible DTN schedules are studied, one is obtained without restrictions to battery utilization, and another with battery constraints in terms of a simplistic LiBaM, using the MILP model with battery parameters listed on Table III. A 10% safety margin is added to the minimal battery charge at all times in order to account for the idealistic nature of the LiBaM. Both resulting schedules are illustrated in Figure 7 and 8 respectively. The schedule with battery awareness forces the network to distribute the utilization of communication resources in space and time resulting in a less concentrated

Table III  
BATTERY MODEL PARAMETERS

	Absolute	Relative
Total battery capacity	277056.0 J	100 %
Initial battery charge	221644.8 J	80 %
Minimal battery charge at all times	166233.0 J	50 + 10 %
Background consumption rate	4.630 J/s	0.001671 %/s
Tx/Rx consumption rate	13.651 J/s	0.004927 %/s
Recharge by sunlight exposure rate	15.472 J/s	0.005584 %/s

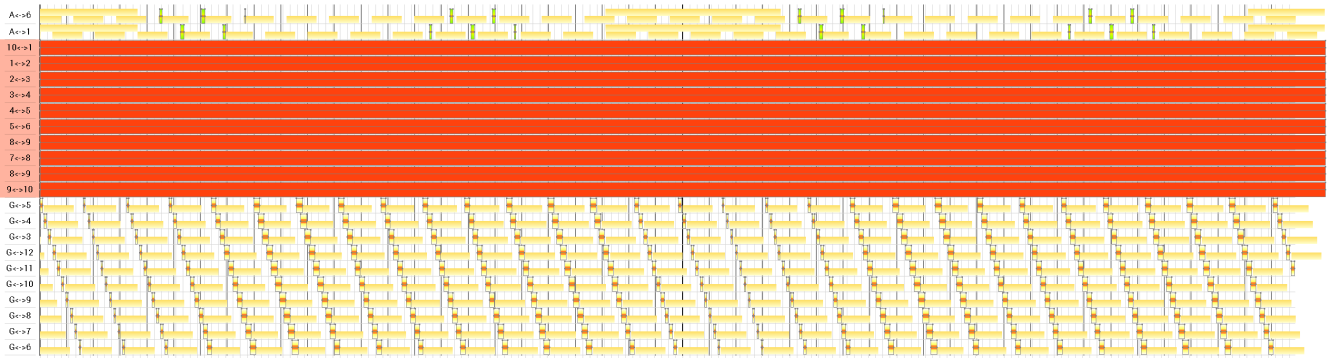


Figure 5. Ulloriaq topology. Abscissas axis is time, ordinates are nodes pairs. Inter-satellite links (in red) could be permanently enabled as satellites are in continuous range of the front and back neighbors. On the top, transmission opportunities (contacts) are plotted for satellite 1 and 6 to Aalborg ground station (A). On the lower part, several visibility opportunities are possible between Greenland territory (G) and each of the 10 satellites. Sunlight exposures for each node are highlighted with a yellow background and black vertical lines divides the time axis in a per-hour scale for a total of 48 hs.

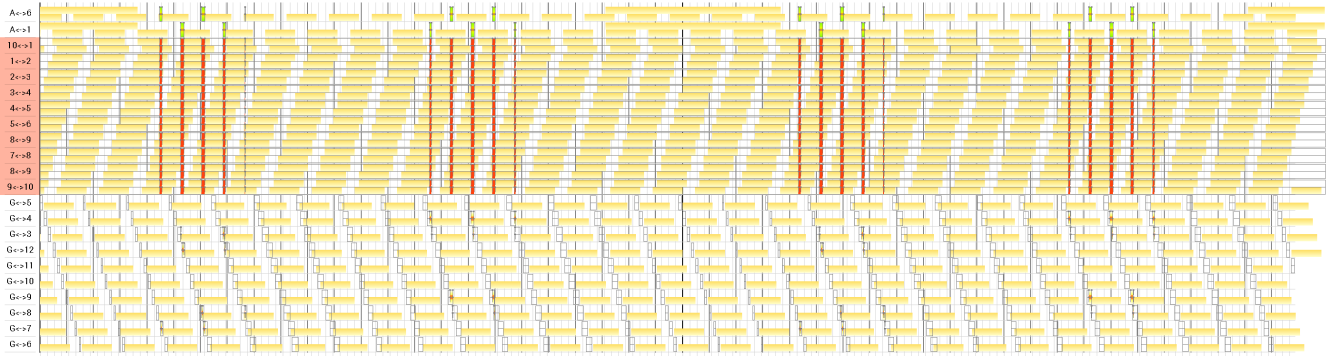


Figure 6. Contact plan with direct end-to-end paths (i.e., no store-carry-and-forward) between Greenland and Aalborg. Data transfers only happens when a chain of links can be established from Aalborg to Greenland. Although the HSL allows for 100 Mbps, the lowest data rate (10 kbps) becomes the bottleneck.

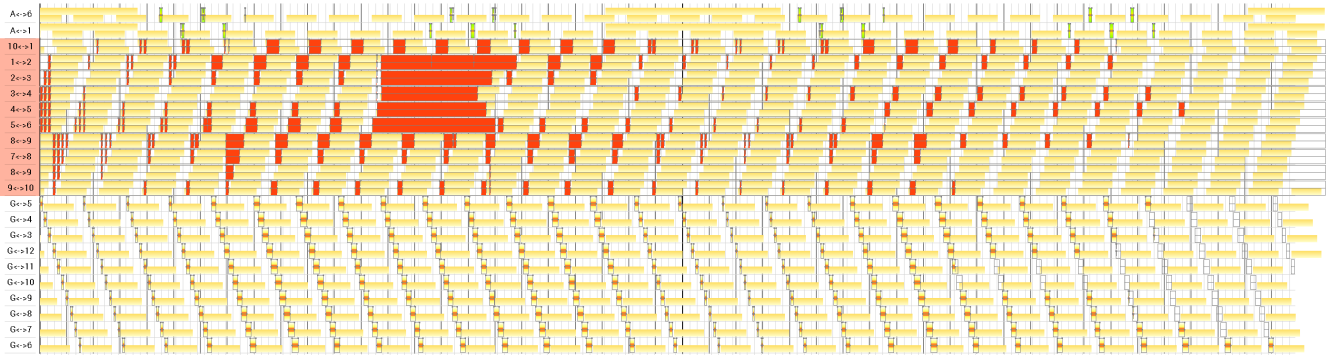


Figure 7. DTN contact plan without battery awareness. Inter-satellite links resources are better utilized and allows a large data collection over Greenland. However, transponder utilization are largely concentrated as the model has no sensitivity towards battery utilization.

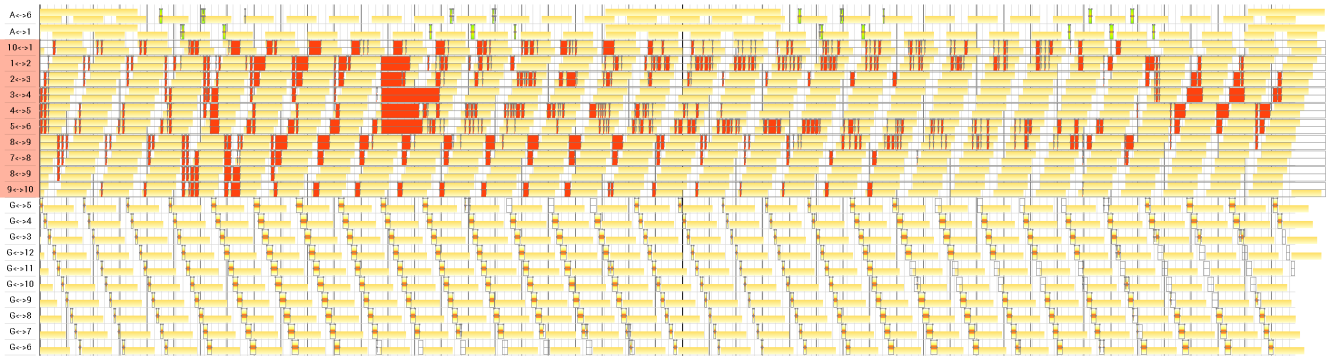


Figure 8. DTN contact plan with battery awareness. Inter-satellite links are further distributed by the LiBaM battery constraints. The resulting contact plan reduces the overall throughput but minimizes the probability of exhausting satellites' batteries.

Table IV  
DATA DELIVERED IN 48 HS

Schedule	Delivered Data
Real-time contact with Greenland (Figure 6)	7.9 MBytes
Battery-agnostic store-carry-and-forward (Figure 7)	186.5 MBytes
Battery-aware store-carry-and-forward (Figure 8)	182.8 MBytes

contact plan than the battery-agnostic one. This is particularly noticeable in the inter-satellite link assignment (red colored schedule). The total delivered data of each of these link schedules are summarized in Table IV.

To analyze the battery utilization, and in particular the risk of dropping below a certain state of charge threshold, we validated the contact plans with respect to the closer-to-reality stochastic KiBaM with parameters  $c = 0.5$  and  $p = 0.0005$ . The uncertainty model around the initial state of charge  $a(0), b(0)$  is truncated Gaussian with a support ranging  $[-4\%, 4\%]$  in both the available and the bound charge dimensions. We additionally assume piecewise truncated white noise around the loads with support of  $[-0.5, 0.5]$  J/s.

The risk of dropping below a safe battery threshold of 50% for each satellite involved in the battery-agnostic contact plan is summarized in Table V. In a battery-agnostic context we see that half of the satellites drop below a critically low state of charge level with certainty, while the battery-aware contact plan causes the satellites to reach such an undesired area with a probability of around 25% at worst. Most satellites exhibit a negligible risk ( $\leq 1\%$ ) of attaining critically low battery levels.

Table V  
THE RISK OF DROPPING BELOW A STATE OF CHARGE THRESHOLD OF 50% IN THE BATTERY-AGNOSTIC CONTACT PLAN OF FIGURE 7 AND THE BATTERY-AWARE CONTACT PLAN OF FIGURE 8.

Satellite Id	Depletion Risk [%]	
	Battery-agnostic	Battery-aware
1	100	25.14
2	100	$1.45 \cdot 10^{-11}$
3	100	0
4	100	0
5	100	$4.44 \cdot 10^{-9}$
6	100	0.98
7	41.12	0
8	0	0
9	0	0
10	0	0

Figure 9 depicts the state of charge evolution of satellite 5 in the battery-aware as well as the battery-agnostic setting. Each plot consist of two subplots, (i) Several KiBaM evolutions on top, showing the most optimistic and the most pessimistic evolution (dashed lines) as well as the mean evolution (solid), and (ii) the load sequence entailed by the contact plan on the bottom. The mean evolution is the KiBaM counterpart to the LiBaM evolution computed in the MILP; with an initial state of charge of  $a(0) = 80\%$  and  $b(0) = 80\%$ , we track its evolution along the load sequence induced by the contact plan. The best case is computed by slightly overapproximating

the highest initial state of charge that is supported by the Gaussian uncertainty, i.e.  $a(0) = 80 + 4\%$  and  $b(0) = 80 + 4\%$  and tracking it along the sequence of best-case loads among those that have support in the load noise model, i.e.  $\ell(t) - 0.5$  J/s in every step. The worst case is symmetric to the best case by picking  $a(0) = 80 - 4\%$  and  $b(0) = 80 - 4\%$  and  $\ell(t) + 0.5$  J/s. Thus, the dashed lines span the corridor of reachable (with positive probability) states of charge along time. Consequently, if the corridor never intersects with the region of undesirably low SoCs (red hatched area), depletion is impossible. Similarly, if even the best-case evolution drops

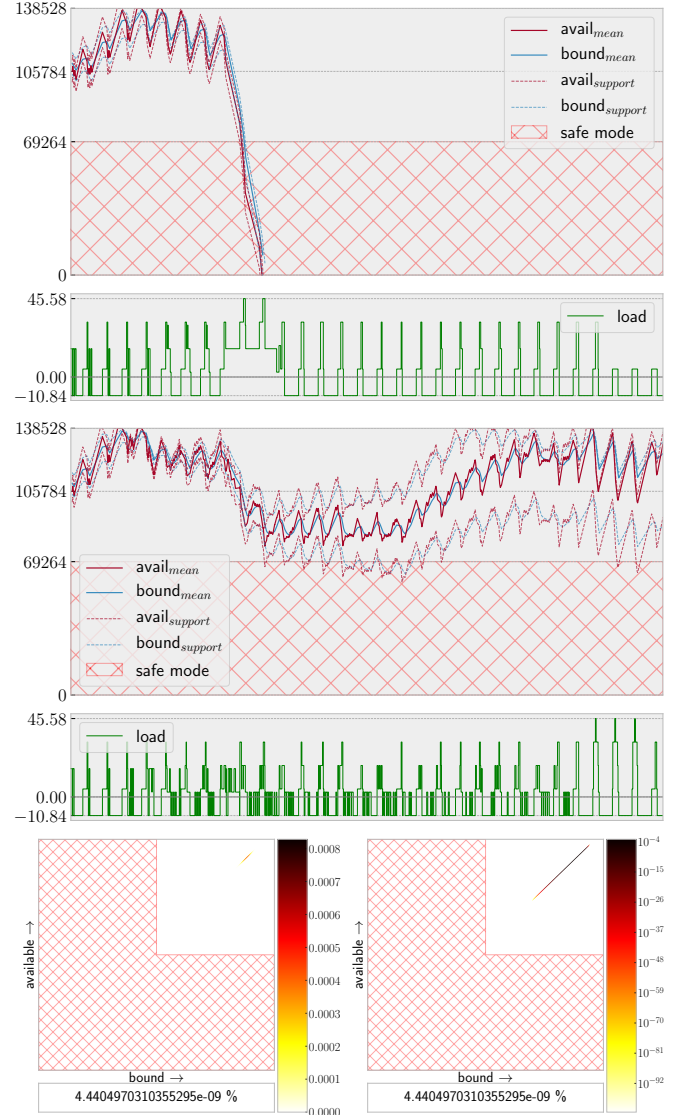


Figure 9. **Top:** The state of charge evolution of satellite 5 in the battery-agnostic plan. The battery-agnostic plan exhibits early certain depletion. Its load profile shows concentrated periods of high load. **Middle:** The corresponding battery-aware contact plan. It induces a much more spread out load profile. Even though its worst-case evolution exposes a risk of depletion, the improvement with respect to the battery-agnostic plan is obvious. **Bottom:** The final SoC distribution of the quantitative validation of the battery-aware plan on a linear (left) as well as on a logarithmic (right) color scale, revealing a negligible depletion risk.

below that threshold, the satellite surely depletes. The borderline, and most interesting case is if the worst-case evolution drops below the threshold but the best-case does not. In this case, we need to quantify the depletion risk by tracking the whole state of charge distribution over time, as explained at the end of Section II-B.

#### A. Discussion

a) *Discretization*: The MILP model captures the time evolution of the topology in  $K$  discrete time intervals and decisions on resources utilization are thus limited to such intervals. However, the fact that Ulloriaq satellites stay in reach of each other continuously render a time-continuous scheduling possible. Moving to a finer-grain discretization, by slitting long intervals into smaller ones, can improve the scheduling at the expense of higher processing effort in solving a larger and more complex model<sup>1</sup>. Exploring optimal discretization of intervals or alternative time-continuous strategies is an appealing future research area in the battery-aware planning.

b) *Model Accuracy*: We analyzed the generated contact plan with the more realistic stochastic KiBaM model as an a-posteriori validation. Indeed, contact plans complying with a linear battery model might need to be rejected in case of non-negligible depletion risk determined by more accurate models. In our case study, a safety-margin of 10% turned out to deliver satisfactory results. Nonetheless, to successfully tackle general cases, a heuristic approach that iteratively finds optimal margins for each scenario seems worthwhile to be considered for future battery-aware contact planning.

c) *Real-Time Traffic*: Store-carry-and-forward was studied as a more flexible approach that allows to conveniently decide on transponder duty cycle and thus on battery utilization. However, in the future Ulloriaq mission, real-time traffic would need to be also considered in the model and treated with priority when a direct connection to Greenland is possible from Aalborg. The remaining capacity can then be used for higher latency data. Although including traffic priorities is possible in state-of-the-art DTN protocols, properly modeling this phenomenon in the proposed MILP model is left as a continuation and extension of this work.

d) *Other means of contact plan synthesis*: Other methods of temporal planning and constraint solving could be used to synthesize battery-aware contact plans. The formalism of *Timed Automata* or its *Priced* extension have been applied numerous times to a variety of scheduling problems. The recently emerging field of *Optimization Modulo Theories* (OMT), an extension of the well-known *Satisfiability Modulo Theories* (SMT) problem, provides a similar formulation of contact plan synthesis than MILP. Several (potentially conflicting)

<sup>1</sup>As a reference, solving the battery-aware MILP model on the Ulloriaq scenario took around 2 hours on a Intel i7-5820K processor at 3.30GHz with 32GB of RAM using IBM CPLEX solver. Given that several contact plans with evaluation periods longer than 48 hs might have to be calculated and evaluated, time can become a critical issue when planning future Ulloriaq constellation with battery-awareness.

objective functions can be optimized with descending priority in order to account for multiple goals.

#### IV. CONCLUSION

The power budget of small-satellites such as GOMX-4A and B are very demanding when considered for networked constellations. A permanent communication link is not to be sustainable only for bounded periods. As a result, we have investigated the utilization of store-carry-and-forward approach to optimize data delivery and battery utilization.

By means of a MILP model, optimal contact plans in terms of data delivery volume and time were determined. By including linear battery constraints, the designed contact plans also allowed to minimize the probability of battery exhaustion in power-constrained satellites. We found that a 10% safe-margin was enough to meet the battery charge conditions as calculated by realistic state-of-the-art battery models.

Demonstrated by the results of a first realistic case study inspired in a potential Ulloriaq constellation, the battery-aware contact plan design is envisioned as a valuable scheduling procedure to make an optimal use of resources in future networked small-satellite constellations.

#### ACKNOWLEDGEMENT

This research has received support from the ERC through Advanced Grant 695614 (POWVER).

#### REFERENCES

- [1] J. Alvarez and B. Walls, "Constellations, clusters, and communication technology: Expanding small satellite access to space," in *2016 IEEE Aerospace Conference*, March 2016, pp. 1–11.
- [2] V. Cerf, S. Burleigh, A. Hooke, L. Torgerson, R. Durst, K. Scott, K. Fall, and H. Weiss, "Delay-tolerant networking architecture," Internet Requests for Comments, RFC Editor, RFC 4838, April 2007, <http://www.rfc-editor.org/rfc/rfc4838.txt>. [Online]. Available: <http://www.rfc-editor.org/rfc/rfc4838.txt>
- [3] J. A. Fraire and J. M. Finochietto, "Design challenges in contact plans for disruption-tolerant satellite networks," *IEEE Communications Magazine*, vol. 53, no. 5, pp. 163–169, May 2015.
- [4] J. A. Fraire, P. G. Madoery, and J. M. Finochietto, "On the design and analysis of fair contact plans in predictable delay-tolerant networks," *IEEE Sensors Journal*, vol. 14, no. 11, pp. 3874–3882, Nov 2014.
- [5] J. A. Fraire and J. Finochietto, "Routing-aware fair contact plan design for predictable delay tolerant networks," *Ad Hoc Networks*, vol. 25, no. PB, pp. 303–313, Feb. 2015. [Online]. Available: <http://dx.doi.org/10.1016/j.adhoc.2014.07.006>
- [6] J. A. Fraire, P. G. Madoery, and J. M. Finochietto, "Traffic-aware contact plan design for disruption-tolerant space sensor networks," *Ad Hoc Networks*, vol. 47, pp. 41 – 52, 2016. [Online]. Available: <http://www.sciencedirect.com/science/article/pii/S1570870516301032>
- [7] D. Zhou, M. Sheng, X. Wang, C. Xu, R. Liu, and J. Li, "Mission aware contact plan design in resource-limited small satellite networks," *IEEE Transactions on Comms.*, vol. 65, no. 6, pp. 2451–2466, June 2017.
- [8] M. Bisgaard, D. Gerhardt, H. Hermanns, J. Krčál, G. Nies, and M. Stenger, "Battery-aware scheduling in low orbit: The gomx-3 case," in *FM 2016: Formal Methods*. Cham: Springer International Publishing, 2016, pp. 559–576.
- [9] G. Nies, M. Stenger, J. Krčál, H. Hermanns, M. Bisgaard, D. Gerhardt, B. Haverkort, M. Jongerden, K. Larsen, and E. Wognsen, *Mastering Operational Limitations of LEO Satellites - The GOMX-3 Approach*. International Astronautical Federation, 9 2016, pp. 1–15.
- [10] M. R. Jongerden and B. R. Haverkort, "Which battery model to use?" *IET Software*, vol. 3, no. 6, pp. 445–457, 2009. [Online]. Available: <http://dx.doi.org/10.1049/iet-sen.2009.0001>

- [11] H. Hermanns, J. Krčál, and G. Nies, "How is your satellite doing? battery kinetics with recharging and uncertainty," *Leibniz Transactions on Embedded Systems*, vol. 4, no. 1, pp. 04–1–04:28, 2017. [Online]. Available: <http://ojs.dagstuhl.de/index.php/lites/article/view/LITES-v004-i001-a004>
- [12] J. A. Fraire, "Introducing contact plan designer: A planning tool for dtn based space terrestrial networks," in *6th International Conference on Space Mission Challenges for Information Technologies (SMC-IT), STINT-DEMO Workshop*, Alcalá de Henares, Spain, Sept. 2017.